BNL-101914-2014-TECH

AD/RHIC/2;BNL-101914-2013-IR

Intrabeam Scattering for a Beam of Gold Ions

G. Parzen

June 1984

Collider Accelerator Department

Brookhaven National Laboratory

U.S. Department of Energy

USDOE Office of Science (SC)

High Energy Facilities
Advanced Projects

BNL
RHIC-2

BROOKHAVEN NATIONAL LABORATORY
Associated Universities, Inc.
Upton, New York 11973

RHIC Technical Note No. 2

INTRABEAM SCATTERING FOR A BEAM OF GOLD IONS

G. Parzen

June 26, 1984

Introduction

This note presents the results for the effects of intrabeam scattering on the longitudinal and transverse beam dimensions for a beam of Au nuclei at various energies corresponding to $\gamma = 5$ to $\gamma = 100$, and for time periods of up to 10 hours.

Intrabeam scattering is the scattering of the particles in the beam from each other through the Coulomb forces that act between each pair of particles. This causes the beam dimensions to grow both longitudinally and transversely, and results in requirements for the transverse aperture and the RF acceleration system. The beam growth also affects the collider performance, as the instantaneous luminosity will decrease with time.

The Lattice

The lattice used is the RHIC-3 lattice (J. Claus, RHIC proposal). In the focussing regular quadrupoles $\chi_p = 1.39$ m, $\beta_x = 51.4$ m. At the crossing points $\beta_x = .9$ m, $\beta_x = 6.3$ m. The SYNCH output tape for the RHIC-3 lattice was used to provide the actual variations of χ_p, β_x, β_y around the ring for the calculations.

The Initial Beam State

For the initial beam dimensions, the normalized horizontal and vertical emittances were assumed to be $\varepsilon_x = \varepsilon_y = 10\ \pi \times 10^{-6}$ m.r. For the initial longitudinal dimensions, it was assumed that the bunch area was .3 ev-sec/amu for γ smaller than the transition γ, $\gamma = \gamma_t = 26.4$; and for $\gamma > \gamma_t$ the bunch area was assumed to be 1 ev-sec/amu. The rms energy spread, $\delta = (\Delta p/p)$ rms, and the rms bunch length, σ_ℓ, are then computed assuming an RF voltage of $V = 1.2 \times 10^6$ volts and the harmonic number $h = 6 \times 57$.

The initial bunch length $\sigma_{\ell o}$ varies from 99 cms at $\gamma = 7$, down to about 37 cms at $\gamma = 20$ (near the transition γ) and then up again to about 48 cms at $\gamma = 100$. The initial rms energy spread, δ_o, varies from $.75 \times 10^{-3}$ at $\gamma = 7$, up to 4.6×10^{-3} at $\gamma = \gamma_t$ and then down again to $.36 \times 10^{-3}$ at $\gamma = 100$.

The final beam state after 2 or 10 hours is not sensitive to the initial beam state; fairly large changes in the initial beam state tend to change the final state by a comparatively small amount.

t = 10 hr Results (Table I)

Table I lists the initial beam state, δ_o, $\sigma_{\ell,o}$, ε_o and the final beam state δ, σ_ℓ, ε after t = 10 hrs, for various energies, from $\gamma = 7$ to $\gamma = 100$. Also listed are the final rms transverse beam dimension $\sigma_E = \chi_p \delta$, $\sigma_H = \sigma_V$, (σ_E and σ_H are given at the focussing quadrupoles where $\chi_p = 1.39$ m and $\beta = 51.4$), and the 95% beam half-width $2.5\ (\sigma_E + \sigma_H)$.

The horizontal and vertical oscillations are assumed to be fully coupled, and thus $\sigma_H = \sigma_V$ throughout the time the beam is growing.

Luminosity results are also listed in Table I. The luminosity decreases with time because of intrabeam scattering. The following luminosity results

Table I.

γ	7	12	20	30	50	75	100
<u>Initial Beam</u>							
$\delta_o/10^{-3}$	.751	.678	.696	1.26	.643	.452	.359
$\sigma_{\ell o}$ (cms)	98.6	63.3	36.9	45.2	53.2	50.5	47.7
ϵ_o/π (mm.mr)	10	10	10	10	10	10	10
<u>Final Beam</u> t=10 hrs							
ϵ/π (mm.mr)	67.2	44.5	35.8	33.2	27.7	27.8	27.8
$\delta/10^{-3}$	1.45	1.56	1.79	1.98	1.54	1.27	1.09
σ_ℓ (cms)	191	146	95.0	71.2	128	142	146
σ_H (mms)	9.07	5.64	3.92	3.08	2.18	1.78	1.54
$\sigma_E=\chi_p\delta$ (mm)	2.02	2.17	2.49	2.76	2.15	1.77	1.53
<u>Beam Half-Width</u>							
$2.5\ (\sigma_H+\sigma_E)$ (mm)	27.2	19.1	15.7	14.3	10.6	8.70	7.52
$2.5\ \sigma_V$ (mm)	22.7	14.1	9.80	7.70	5.45	4.45	3.85
<u>RF</u>							
$2.5\ \delta/10^{-3}$	3.63	3.91	4.48	4.96	3.87	3.18	2.74
$(\Delta p/p)$ bucket$/10^{-3}$	2.72	3.82	6.72	9.95	4.31	3.19	2.68
<u>Luminosity</u>							
$L_o/10^{26}$	.868	1.49	2.48	3.72	6.20	9.30	12.4
L_{AV}/L_o	.214	.319	.389	.422	.476	.471	.470
$L\ (\alpha=0)/10^{26}$	--	.475	.965	1.57	2.95	4.38	5.83
$L\ (\alpha=2\times10^{-3})/10^{26}$	--	.218	.458	.776	.642	.709	.800

are listed. L_o, the initial luminosity for head-on collisions, L_{AV}/L_o, the average luminosity over 10 hours for head-on collisions divided by L_o, L (α = 0), the average luminosity for head-on collisions, and L (α = 2), the average luminosity for a 2 mr crossing angle. For a period of 10 hours, collider operation appears possible down to about γ= 12. At γ = 7, collider operation appears possible for t = 2 hours, and the luminosity results for γ = 7 are given in Table II. The luminosity results are for 1.2×10^9 ions/bunch.

t = 2 hr Results (Table II)

Table II shows effects of intrabeam scattering over 2 hours. The same results which are listed in Table I are listed in Table II for a time interval of 2 hours instead of 10 hours.

Operation at Low γ, $\gamma < 12$

Below γ = 12, the lifetime of the beam is limited by intrabeam scattering. The first limit one meets is the size of the RF bucket; the $\Delta p/p$ of the beam begins to exceed the maximum $\Delta p/p$ of the bucket. Using as a criteria the time when the energy spread in the beam equals the maximum energy spread of the bucket, one finds that operation at γ = 7 is limited to 2 hours, and at γ = 5 to .65 hours. The results for γ = 7 are given in Table II. For γ = 5, one finds that over .65 hours

$L_o = .62 \times 10^{26}$

$L/L_o = .63$

$L\ (\alpha = 0) = .39 \times 10^{26}$

$L\ (\alpha = 2) = .23 \times 10^{26}$

At $\gamma = 5$, the beam dimensions start at $\delta_o = .818 \times 10^{-3}$, $\sigma_{\ell o} = 128$ cm, $\varepsilon_o/\pi = 10$, and, after .65 hours, grow to $\delta = .93 \times 10^{-3}$, $\sigma_\ell = 145$ cm, $\sigma_H = 8$ mm, $\sigma_E = 1.29$ mm, and beam half-width = 23 mm.

Table II.

γ	7	12	20	30	50	75	100
<u>Initial Beam</u>							
$\delta_o/10^{-3}$	.751	.678	.696	1.26	.643	.452	.359
$\sigma_{\ell o}/10^{-3}$ (cm)	98.6	63.3	36.9	45.2	53.2	50.5	47.7
ε_o/π (mm.mr)	10	10	10	10	10	10	10
<u>Final Beam</u> t=10 hrs							
ε/π (mm.mr)	41.0	27.4	22.4	20.4	18.3	18.5	18.7
$\delta/10^{-3}$	1.14	1.23	1.41	1.60	1.18	.951	.817
σ_ℓ (cm)	149	115	75.0	57.5	97.7	106	109
σ_H (mm)	7.08	4.42	3.09	2.41	1.77	1.45	1.26
$\sigma_E=\chi_p\delta$ (mm)	1.58	1.71	1.97	2.23	1.64	1.32	1.14
<u>Beam Half-Width</u>							
$2.5\ (\sigma_H+\sigma_E)$ (mm)	21.2	15.0	12.4	11.4	8.36	6.80	5.88
$2.5\ \sigma_V$ (mm)	17.7	11.0	7.72	6.02	4.42	3.62	3.15
<u>RF</u>							
$2.5\ \delta/10^{-3}$	2.79	3.08	3.54	4.01	2.95	2.38	2.04
$(\Delta p/p)$ bucket$/10^{-3}$	2.72	3.82	6.72	9.95	4.31	3.19	2.68
<u>Luminosity</u>							
$L_o/10^{26}$	.868	1.49	2.48	3.72	6.20	9.30	12.4
L_{AV}/L_o	.348	.506	.596	.645	.677	.665	.663
$L\ (\alpha=0)/10^{26}$	.302	.753	1.48	2.40	4.20	6.18	8.22
$L\ (\alpha=2\times10^{-3})/10^{26}$	.159	.338	.702	1.15	.969	1.09	1.23

Figures

The following figures show the growth of the beam due to intrabeam scattering. Most of the graphs plot information listed in the two tables. Figure 3 and Figure 8 show the time dependence of the beam halfwidth and the luminosity.

Figure 1

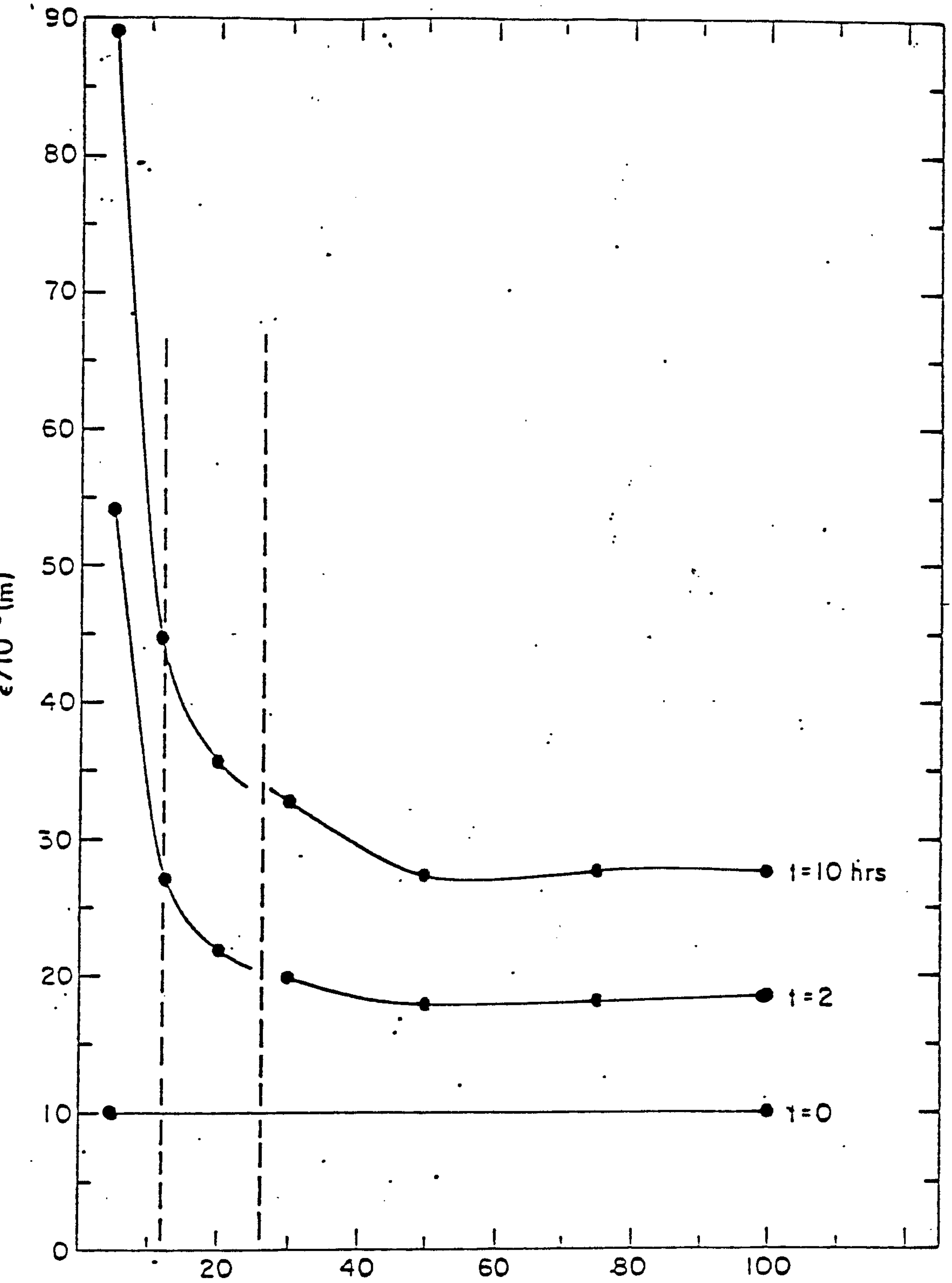

Beam emittance growth due to intra-beam scattering.

Figure 2

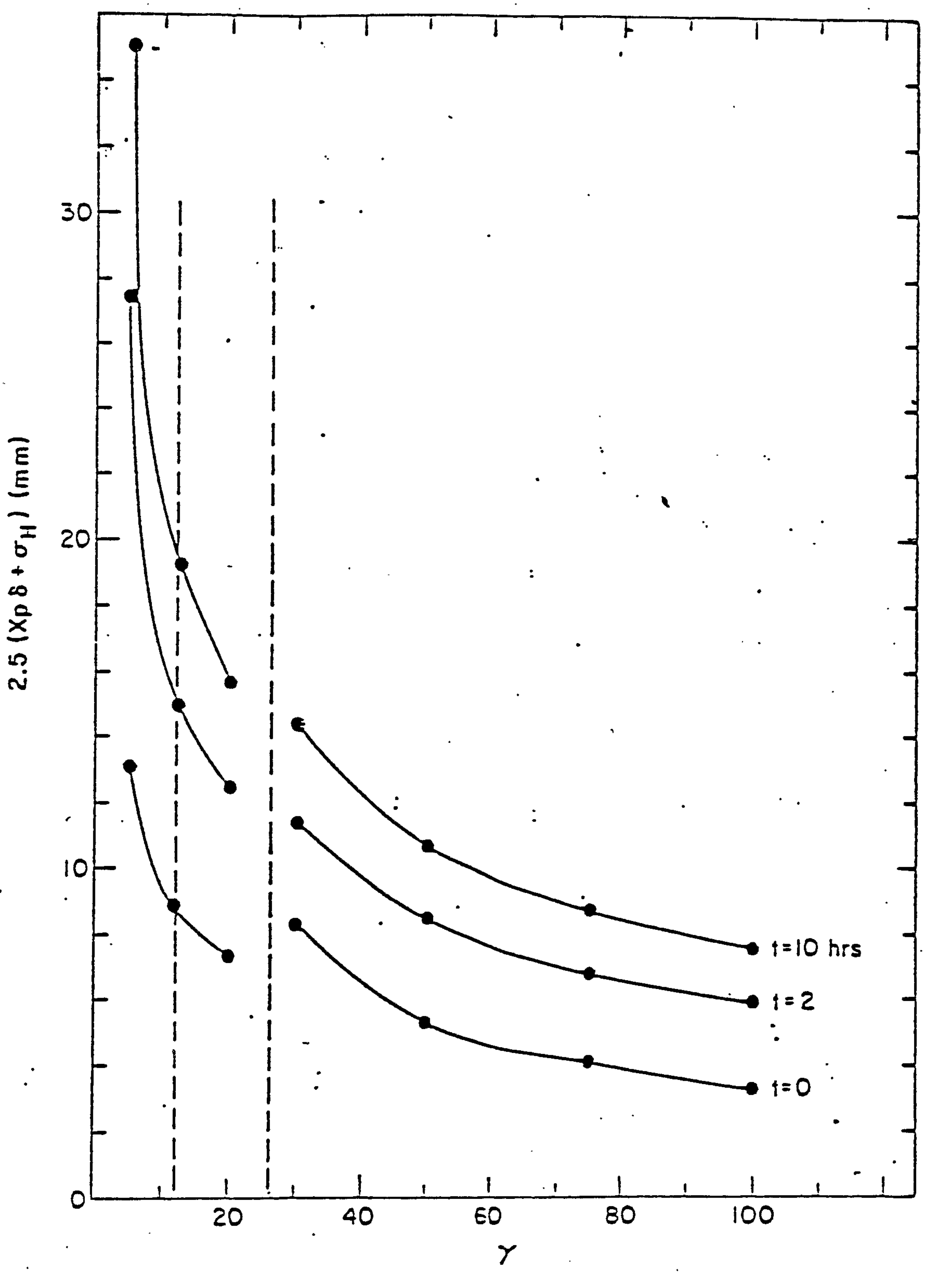

Beam half-width growth due to intra-beam scattering.

Figure 3

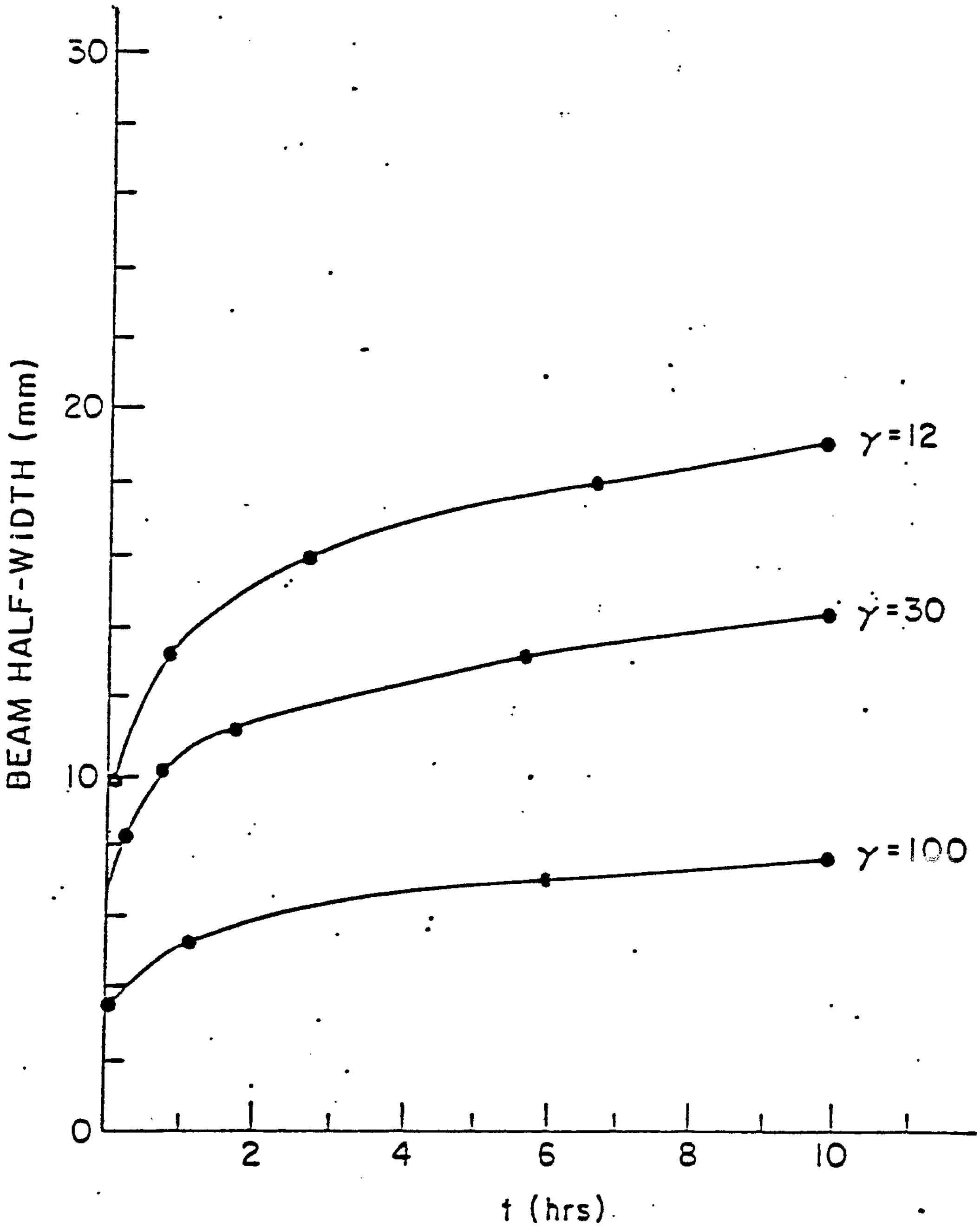

Beam half-width versus time.

Figure 4

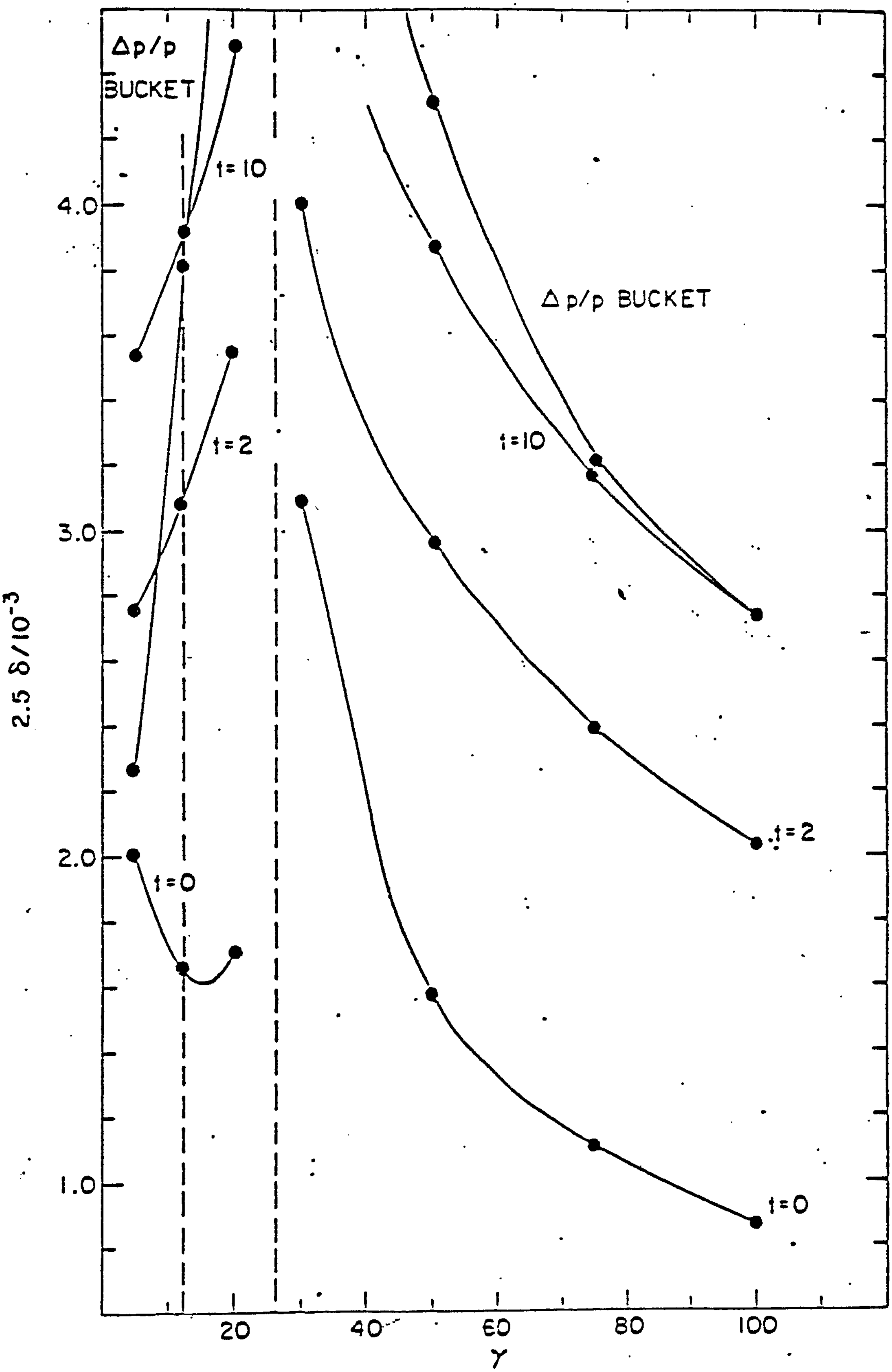

Beam bunch height growth due to intra-beam scattering.

Figure 5

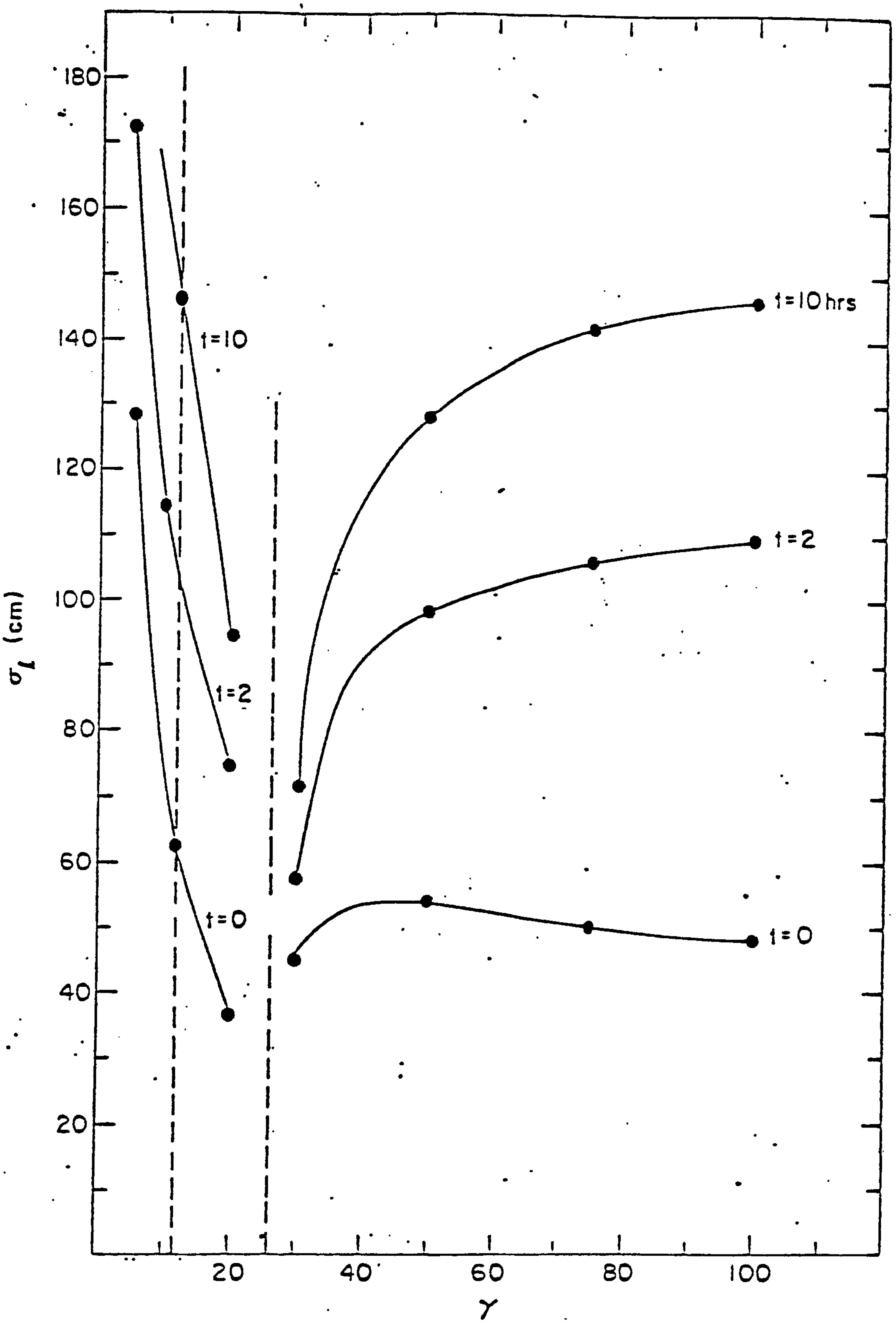

Bunch length growth due to intra-beam scattering.

Figure 6

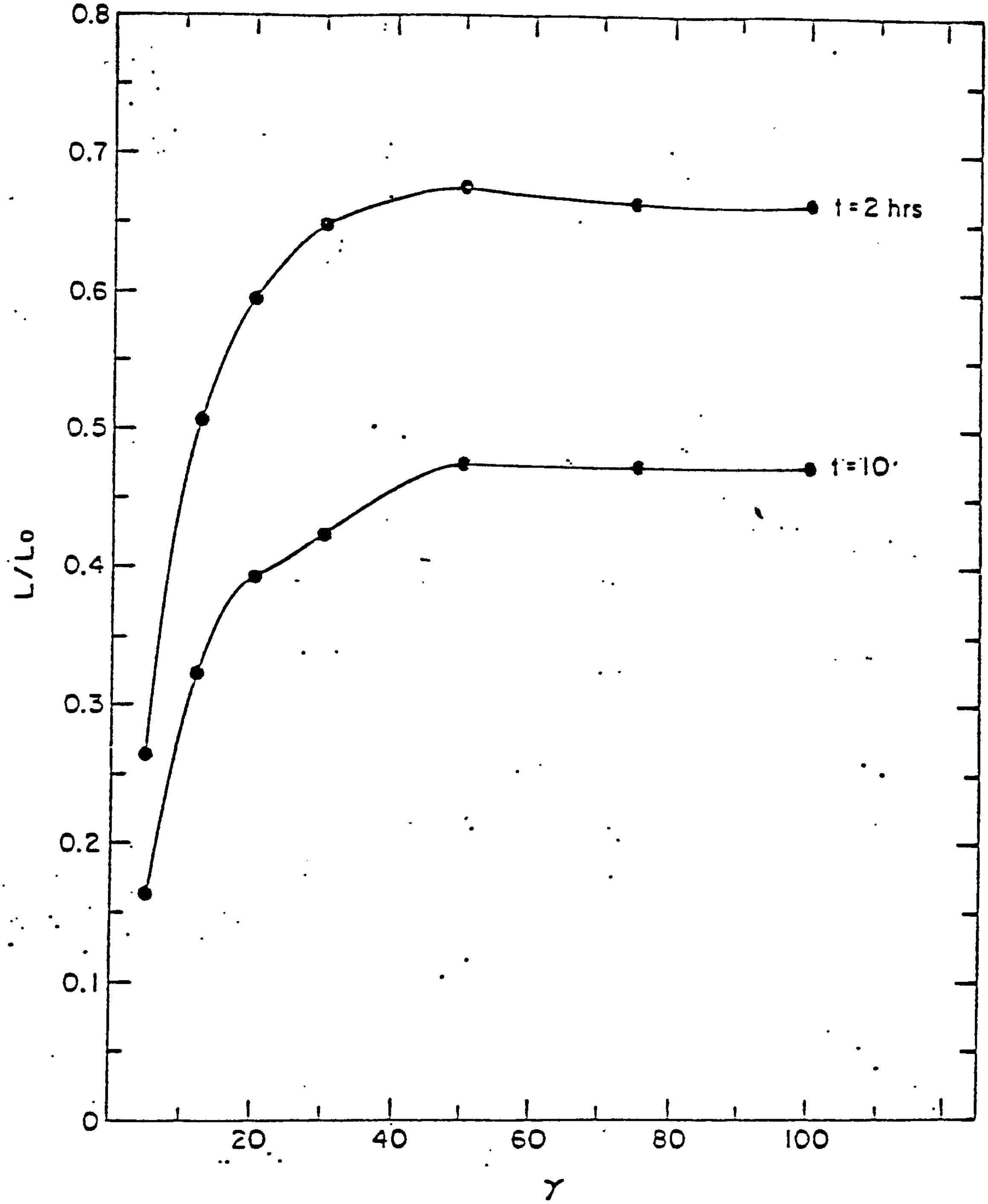

Average luminosity (normalized to its initial value) versus energy for the case of Au on Au, and head-on collisions.

Figure 7

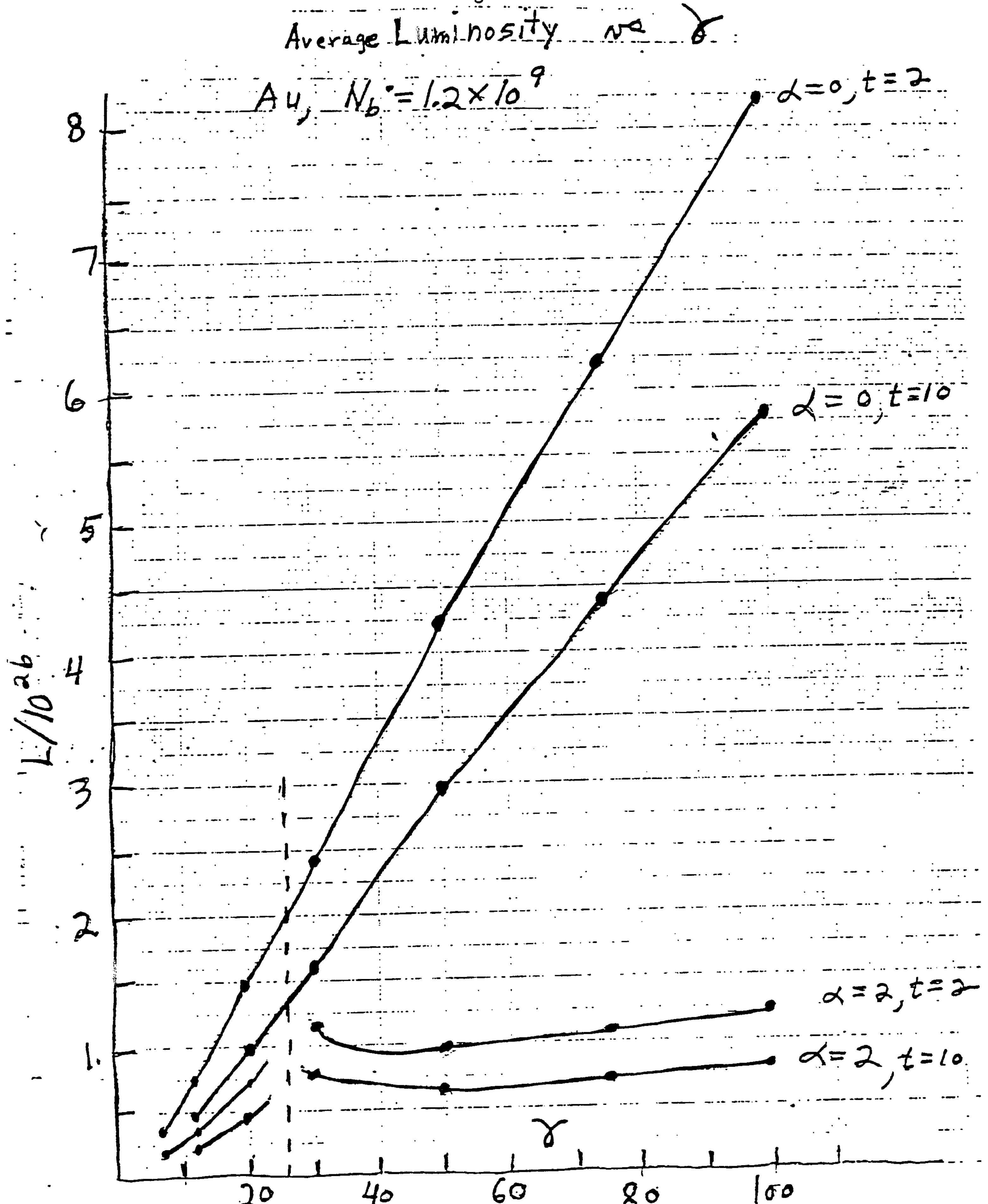
Average Luminosity vs γ
Au, $N_b = 1.2 \times 10^9$
α=0, t=2
α=0, t=10
α=2, t=2
α=2, t=10
L/10^26
γ
1.
2
3
4
5
6
7
8
20
40
60
80
100

Figure 8